

Source Mechanisms of Deep Long Period Earthquakes beneath the Klyuchevskoy Volcano Group inferred from S-to-P amplitude ratios

Natalia Galina^{1,2}, Nikolai Shapiro¹

(1) Institut des Sciences de la Terre, Université Grenoble Alpes,
CNRS, Grenoble, France

(2) Schmidt Institute of Physics of the Earth RAS,
Moscow, Russia

This presentation participates in OSPP



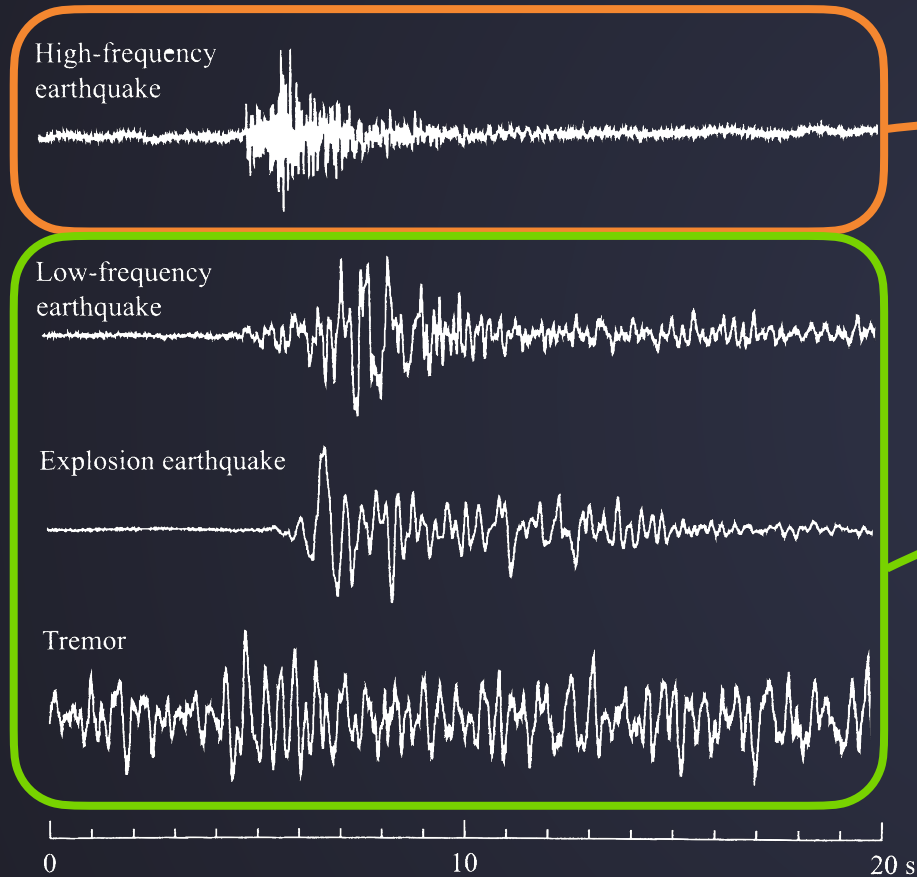
Outstanding Student & PhD
candidate Presentation contest

May 27, 2022



Main classes of volcanic seismicity

Volcano-tectonic earthquakes:
faulting within the solid part of volcanic edifices



Long period (0.5-5 Hz) seismicity:
processes within the magmatic/hydrothermal
system

Mt. Tokachi (Japan)
From Nishimura and Iguchi, 2011

Deep long period seismicity

Although long period (LP) earthquakes and tremor were observed at various volcanoes usually they occurred at shallow depths (< 5 km)

For the first time **deep LP events (DLP)** were registered beneath Mount Pinatubo, Philippines, and linked with its eruption following after earthquakes swarms.

Precursory Deep Long-Period Earthquakes at Mount Pinatubo: Spatio-Temporal Link to a Basalt Trigger

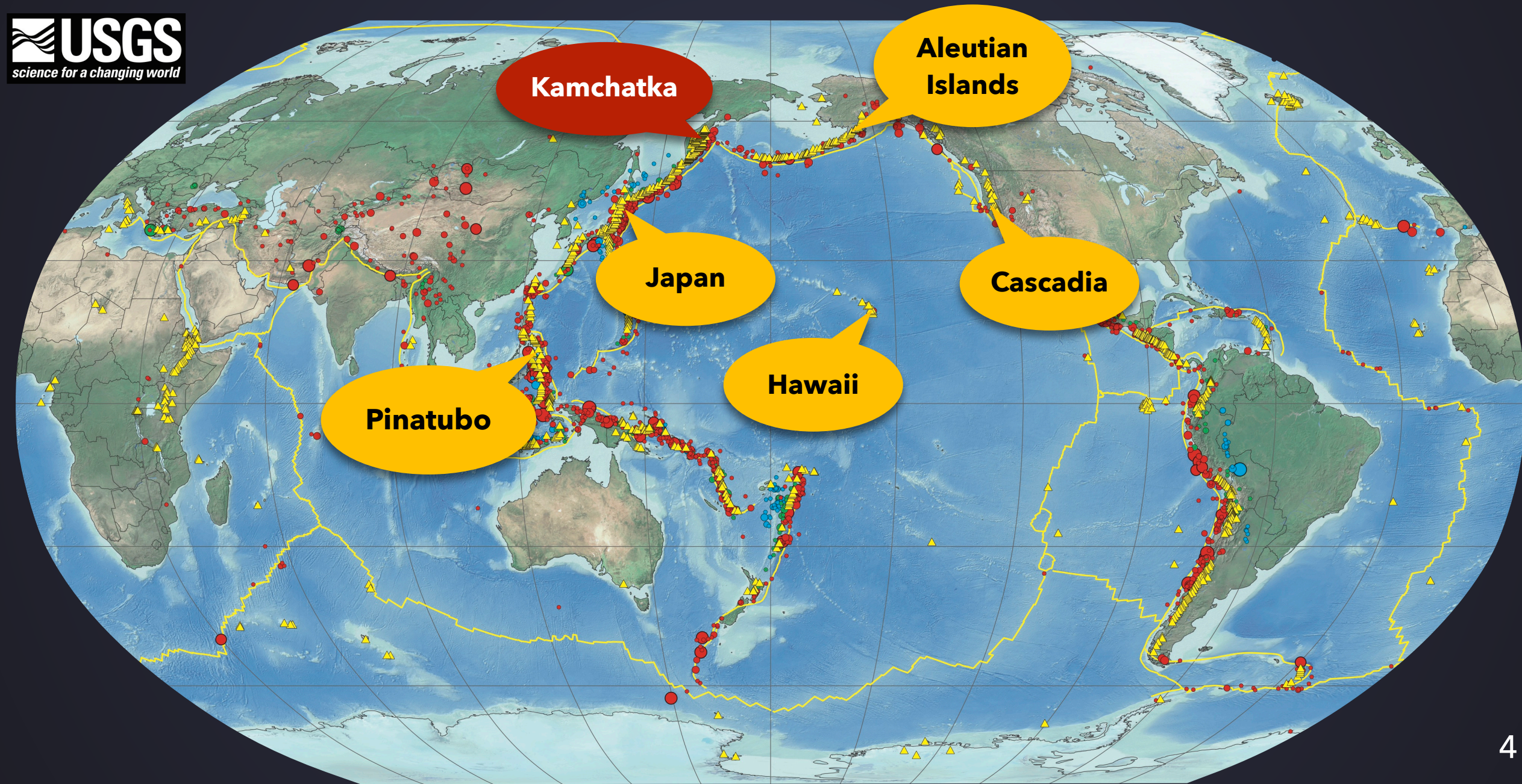
By Randall A. White ¹

¹U.S. Geological Survey.

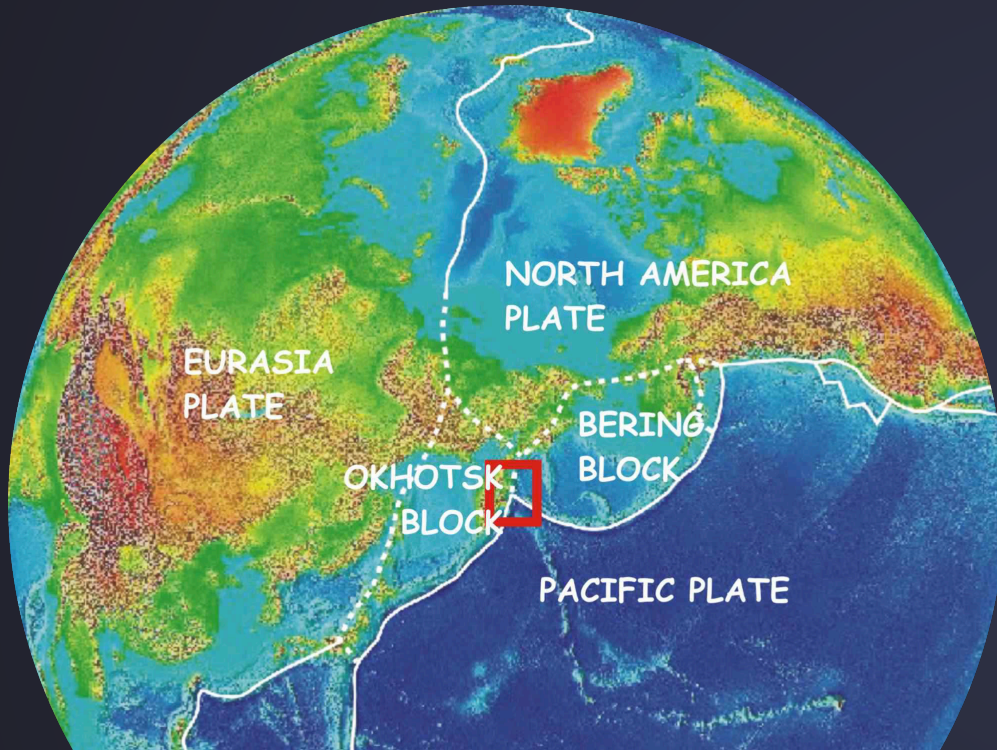
ABSTRACT

About 600 deep long-period (DLP) earthquakes occurred beneath Mount Pinatubo in late May and early June 1991. This number is higher than the combined total number of such earthquakes previously reported at all convergent-margin volcanoes worldwide. The DLP earthquakes occurred in two episodes of roughly similar total energy release, from 1700 May 26 to 1210 May 28 and from 2114 May 31 to 1510 June 8. During these

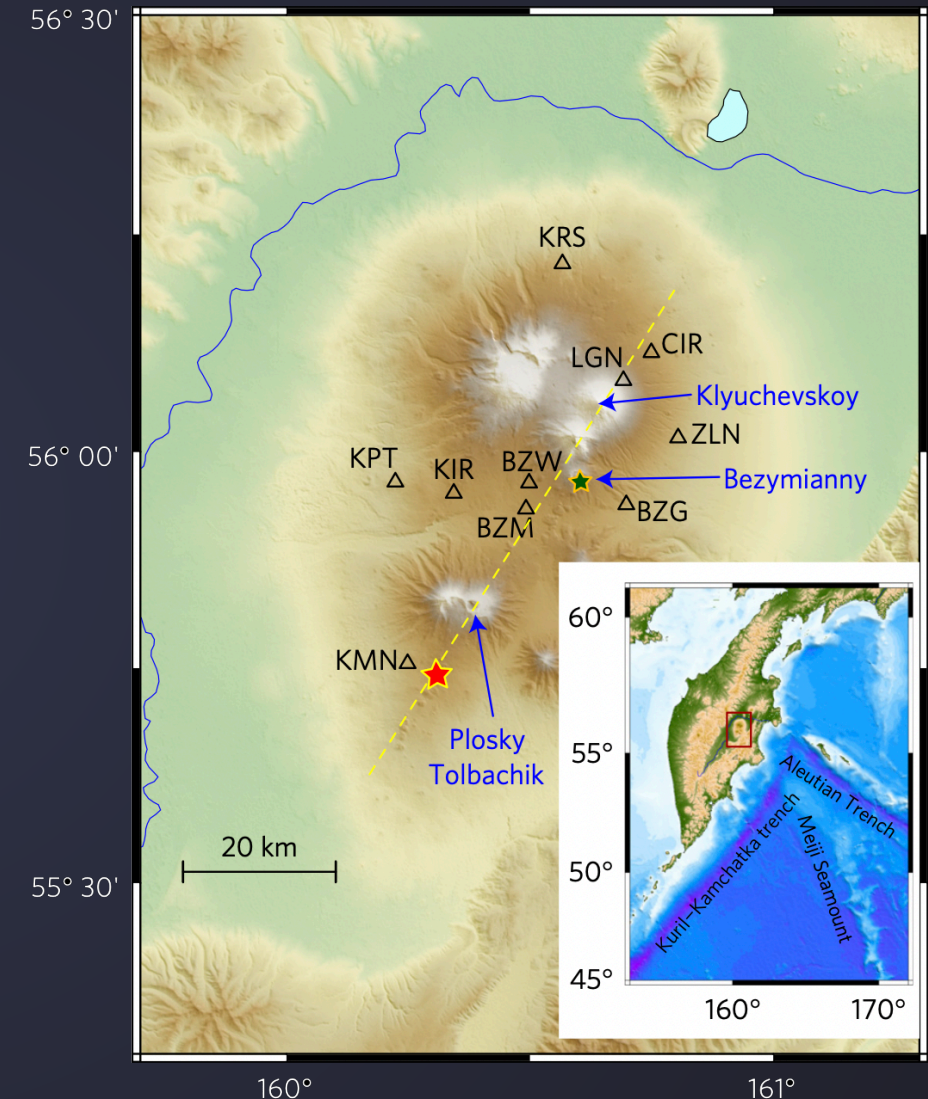
Later DLPs were recorded at numerous volcanoes in different regions



Klyuchevskoy volcano group (KVG) is the natural laboratory for studying long-period seismicity



Kamchatka has a unique tectonic setting, it is an active subduction zone that exhibits intense seismic and volcanic activities



Shapiro, N., Droznin, D., Droznina, S. et al.
Deep and shallow long-period volcanic seismicity linked by fluid-pressure transfer
Nature Geosciences **10**, 442–445 (2017)

The main question:

What is the physical mechanism of DLPs?

They occur in the low crust or at the crust-mantle boundary



Higher temperatures

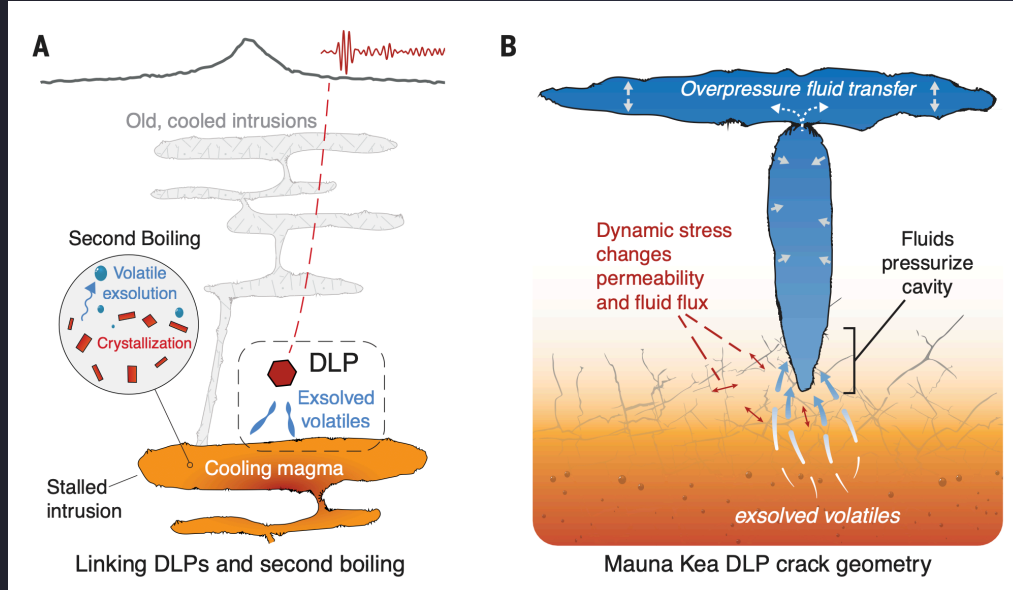


Lower probability of brittle failures

What hypotheses can be assumed in given conditions?

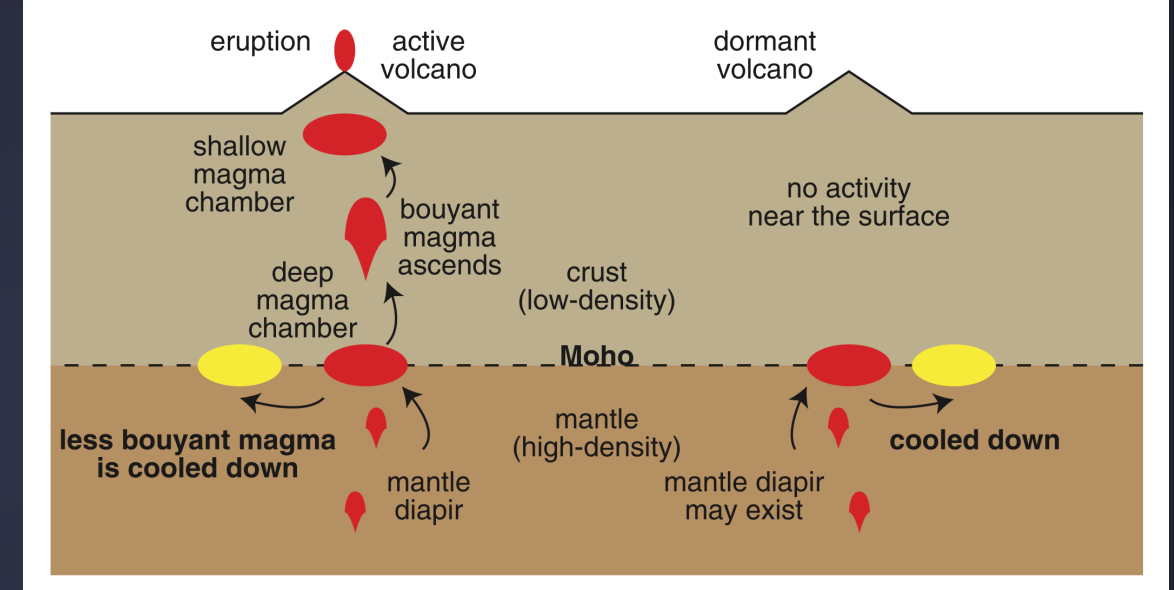
Possible mechanisms of deep long period earthquakes

Second boiling



Aaron G. Wech, Weston A. Thelen, Amanda M. Thomas
Deep long-period earthquakes generated by second boiling beneath Mauna Kea volcano
Science (2020)

Cooling of deep intrusions

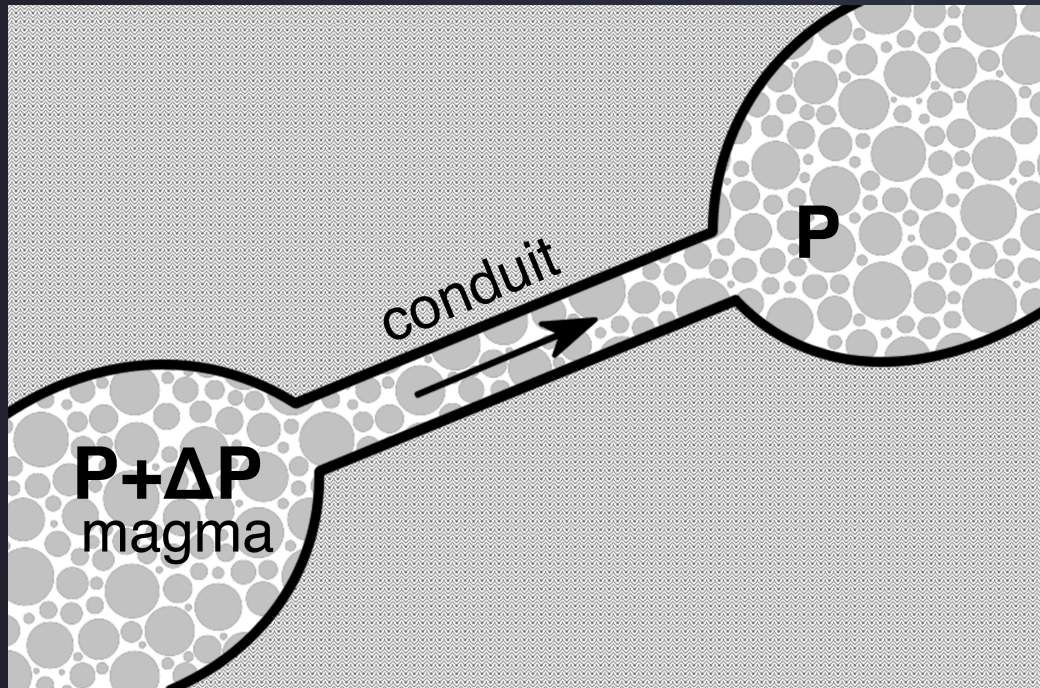


Aso, N., & Tsai, V. C.
Cooling magma model for deep volcanic long-period earthquakes.
Journal of Geophysical Research: Solid Earth (2014)

These models suggest magma cooling what is unlikely to occur in active magmatic system of Kamchatka volcanoes

Processes in volcanic systems and corresponding physical mechanisms

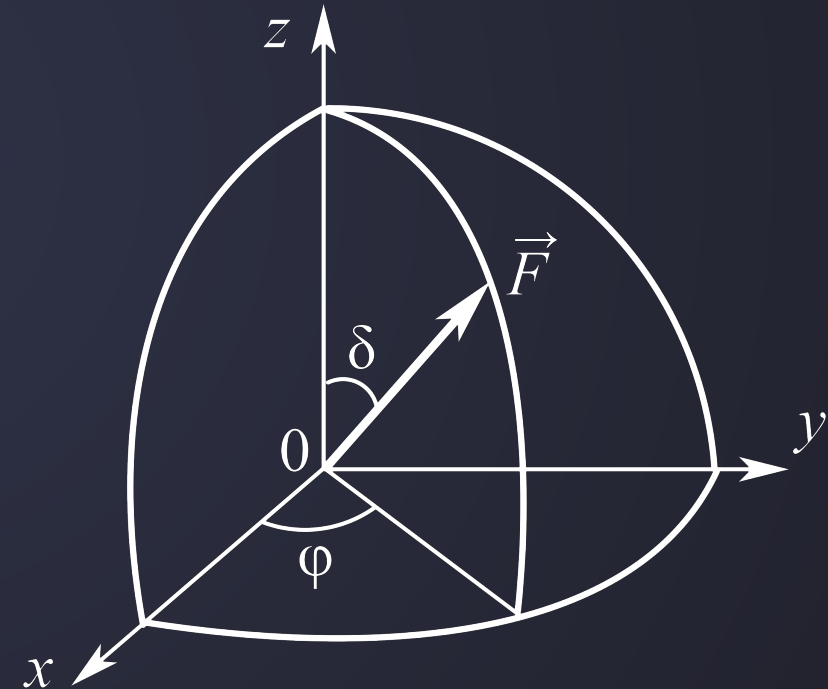
Magma movement upward (downward) in a conduit creates a traction force acting upward on the walls.



A single force

Its orientation can be defined by two angles in a spherical coordinate system

Azimuth $\varphi \in [0^\circ, 360^\circ]$, dip $\delta \in [0^\circ, 90^\circ]$



Ukawa, Motoo, and Masakazu Ohtake

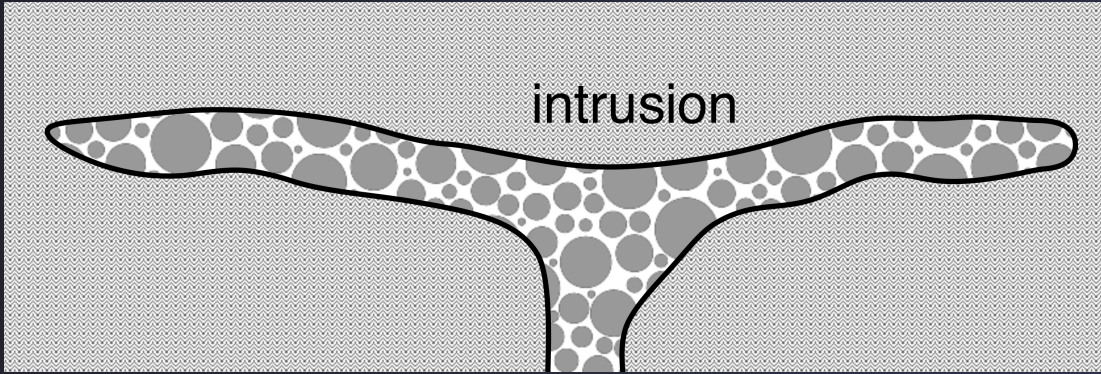
A monochromatic earthquake suggesting deep-seated magmatic activity beneath the Izu-Ooshima Volcano, Japan
Journal of Geophysical Research: Solid Earth (1987)

Processes in volcanic systems and corresponding physical mechanisms

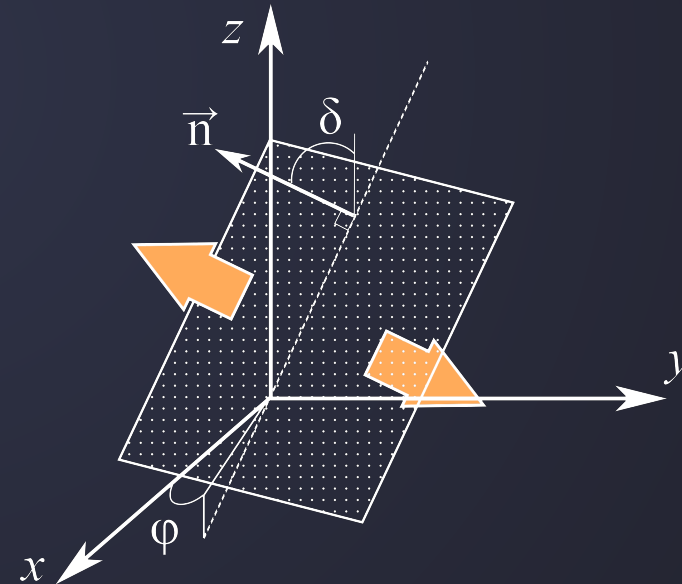
A tensile crack

Its orientation can be defined by two angles as well

$$\varphi \in [0^\circ, 360^\circ], \delta \in [0^\circ, 90^\circ]$$

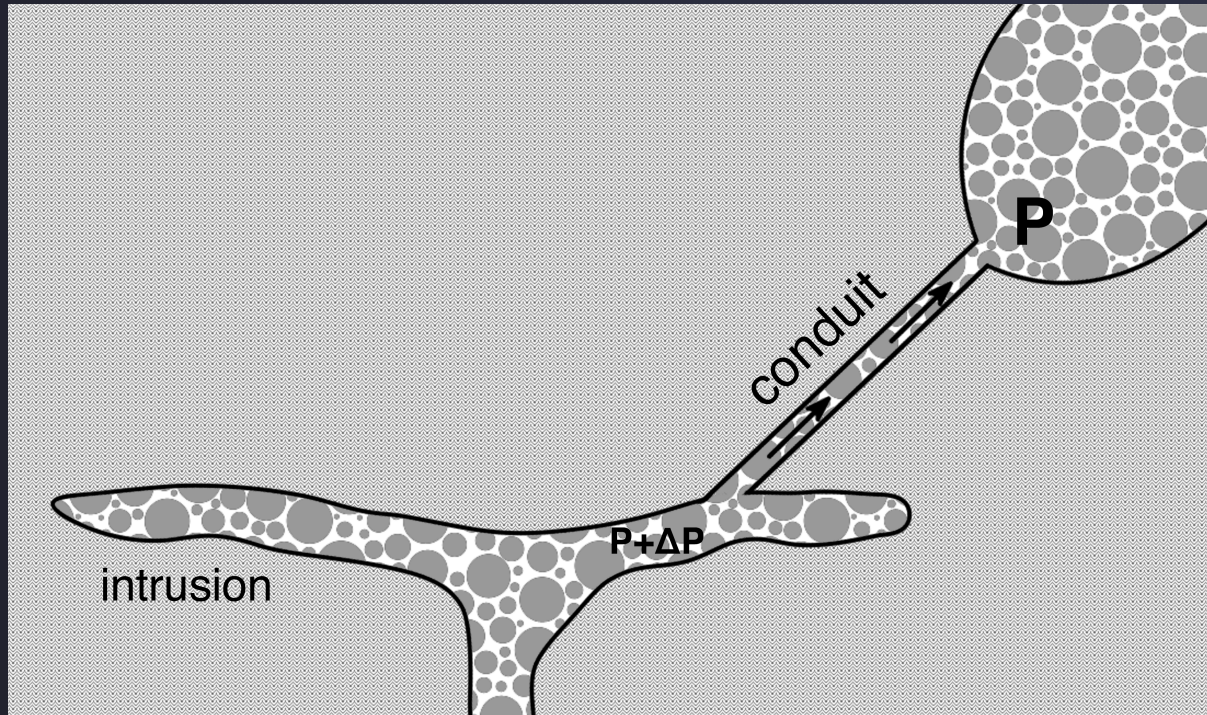


Rapid change of pressure in an intrusion and its following **expansion** due to rapid degassing for example



Processes in volcanic systems and corresponding physical mechanisms

Opening of a sill that causes magma movement in a conduit



A combined source

Consists of a horizontal tensile crack and a single force

Azimuth $\varphi \in [0^\circ, 360^\circ]$

dip $\delta \in [0^\circ, 90^\circ]$

and **ratio** $A_c : A_f$

Processes in volcanic systems and corresponding physical mechanisms

Volcano-tectonic earthquakes linked with **brittle failure** in surrounding rocks

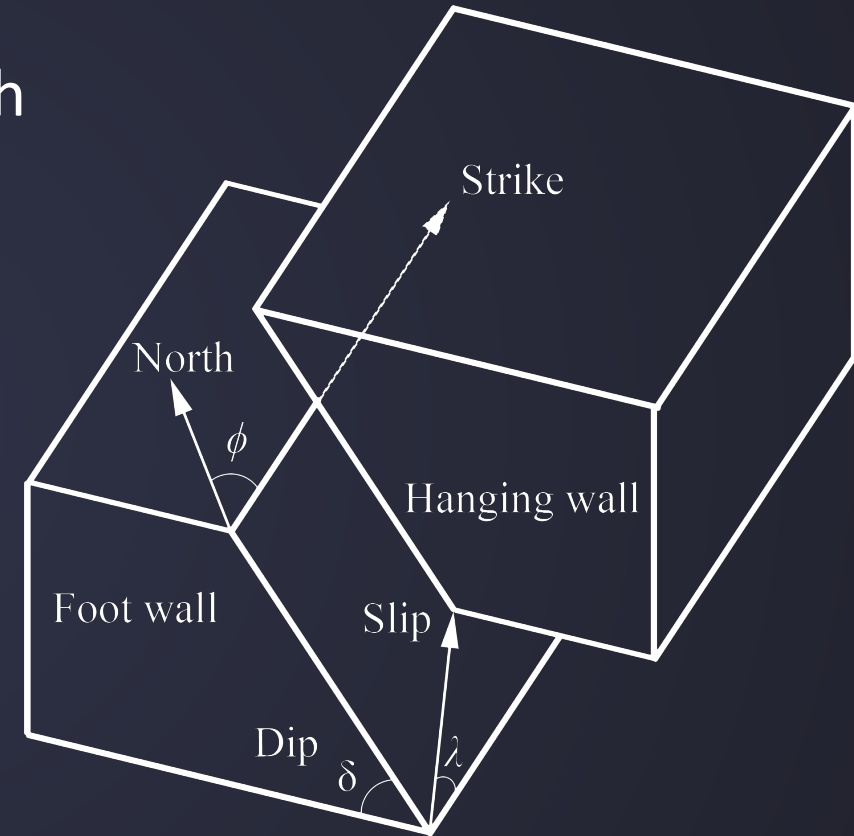
A shear fault

Its orientation is defined by three angles

strike $\phi_S \in [0^\circ, 360^\circ]$

dip $\delta \in [0^\circ, 90^\circ]$

rake $\lambda \in [-180^\circ, 180^\circ]$



Comparison of calculated and real amplitudes

Instead of a widely accepted method with plotting polarities of P-waves arrivals we used the **method of comparison S-to-P amplitude ratios**

Reasons to do it:

1. P-waves onsets for DLPs are too weak
2. Seismograms filtering can inverse polarities

General workflow

1. Measuring real amplitudes of P- and S-waves (A_P , A_S) considering site amplifications
2. Calculation of theoretical P- and S-waves amplitudes for a fixed source orientation
3. Calculating real and theoretical amplitudes ratios

General workflow

1. Measuring real amplitudes of P- and S-waves (A_P , A_S) considering site amplifications
2. Calculation of theoretical P- and S-waves amplitudes for a fixed source orientation
3. Calculating real and theoretical amplitudes ratios
4. Calculating the residuals at each station:

$$\Delta_i = \left| \left(\frac{A_S}{A_P} \right)^{real} - \left(\frac{A_S}{A_P} \right)^{theoretical} \right|$$

5. Obtaining the misfit function as

$$M_{L_1} = \frac{1}{N_{st}} \sum_{i=1}^{N_{st}} \Delta_i$$

General workflow

1. Measuring real amplitudes of P- and S-waves (A_P , A_S) considering site amplifications
2. Calculation of theoretical P- and S-waves amplitudes for a fixed source orientation
3. Calculating real and theoretical amplitudes ratios
4. Calculating the residuals at each station:

$$\Delta_i = \left| \left(\frac{A_S}{A_P} \right)^{real} - \left(\frac{A_S}{A_P} \right)^{theoretical} \right|$$

5. Obtaining the misfit function as

$$M_{L_1} = \frac{1}{N_{st}} \sum_{i=1}^{N_{st}} \Delta_i$$

For a fixed source orientation !

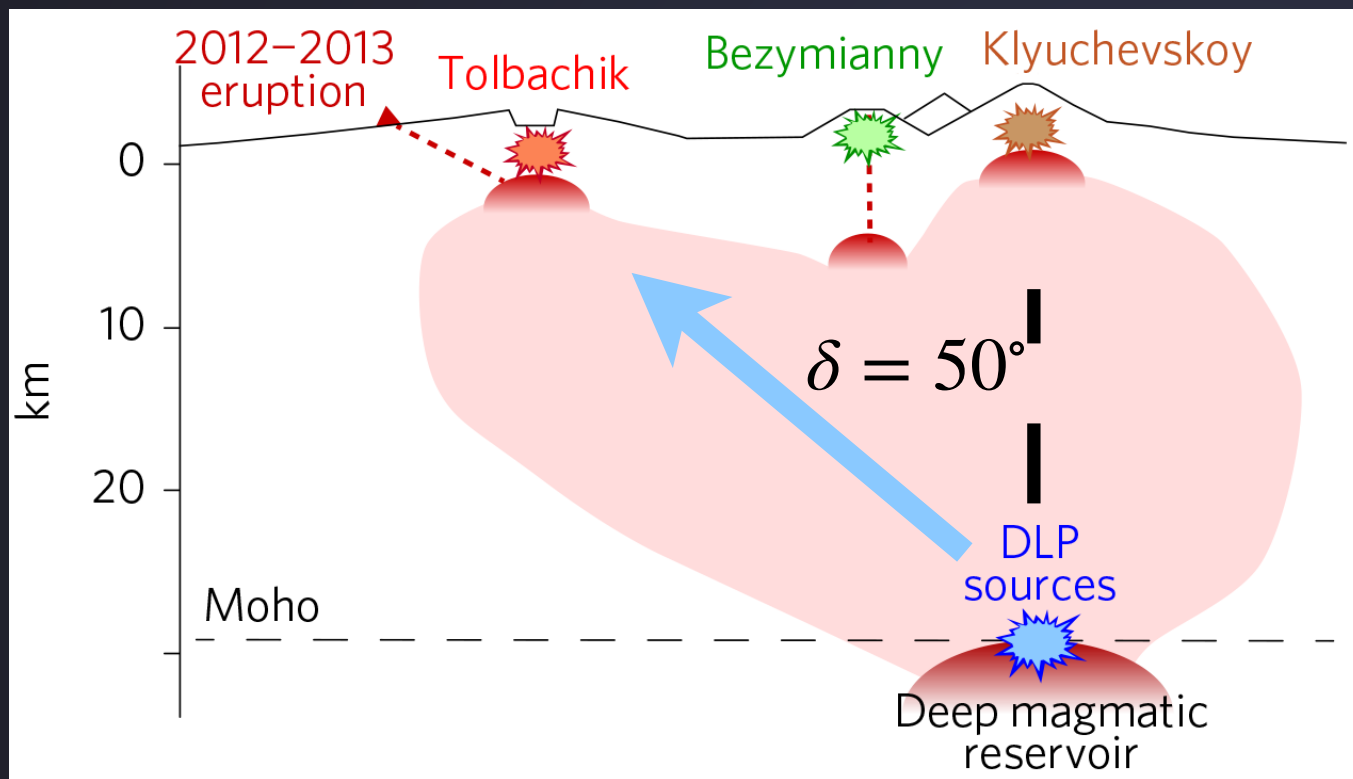
Systematic search over full grid of source parameters (angles) to minimize the misfit function and to find an optimal solution

Results: example DLP on 20 August 2015 at 12:23:54

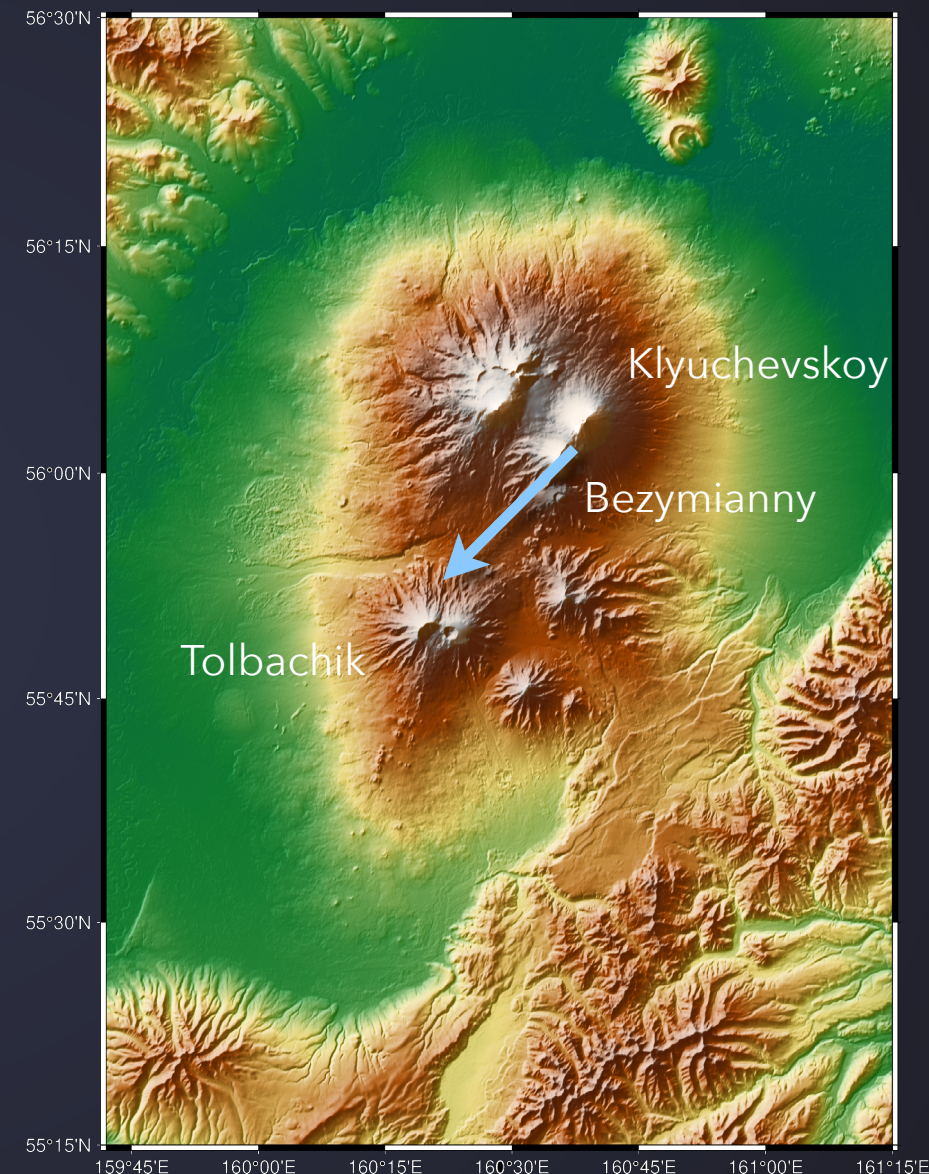
	Force	Shear slip	Tensile crack	Combined source
M_{L_1}	0.92	1.61	0.87	0.72
Source orientation	(220°, 40°)	(335°, 20°, 155°)	(275°, 20°)	(225°, 50°) $A_c : A_f = 1:2$

Possible interpretation

Modified from Shapiro, N. et al.
Nature Geosciences **10**, 442–445 (2017)



**A sill opening with following magma movement
towards Tolbachik volcano**



A dramatic night-time photograph of a volcano erupting. The dark, conical mountain is partially covered in ash and snow. A bright, glowing orange and yellow lava flow is visible on the right side of the slope, cascading down. The sky is a deep, dark blue, filled with numerous small, bright stars. The overall scene is illuminated by the intense light of the eruption, creating a high-contrast, awe-inspiring image.

Thank you !

`nataliya.galina@univ-grenoble-alpes.fr`

Supplementary materials



General workflow

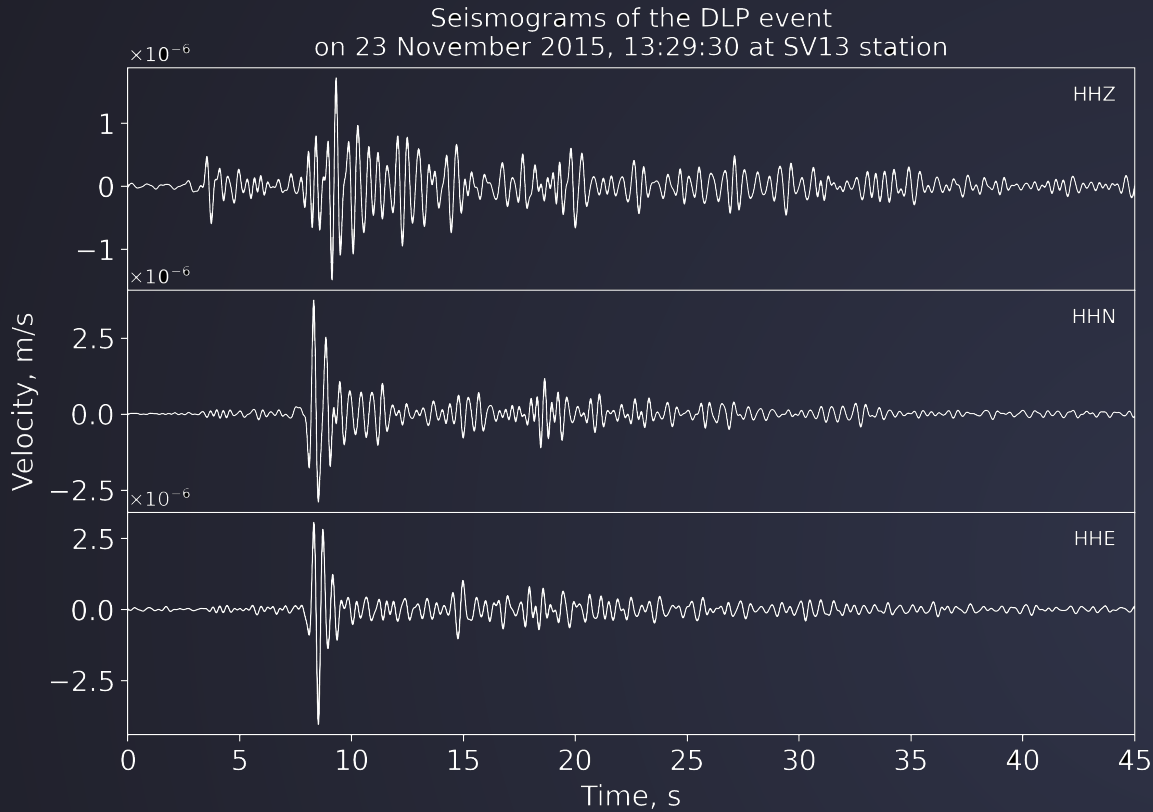
1. Measuring real amplitudes of P- and S-waves (A_P , A_S) considering site amplifications
2. Calculation of theoretical P- and S-waves amplitudes for a fixed source orientation
3. Calculating real and theoretical amplitudes ratios
4. Calculating the residuals at each station:

$$\Delta_i = \left| \left(\frac{A_S}{A_P} \right)^{real} - \left(\frac{A_S}{A_P} \right)^{theoretical} \right|$$

5. Obtaining the misfit function as

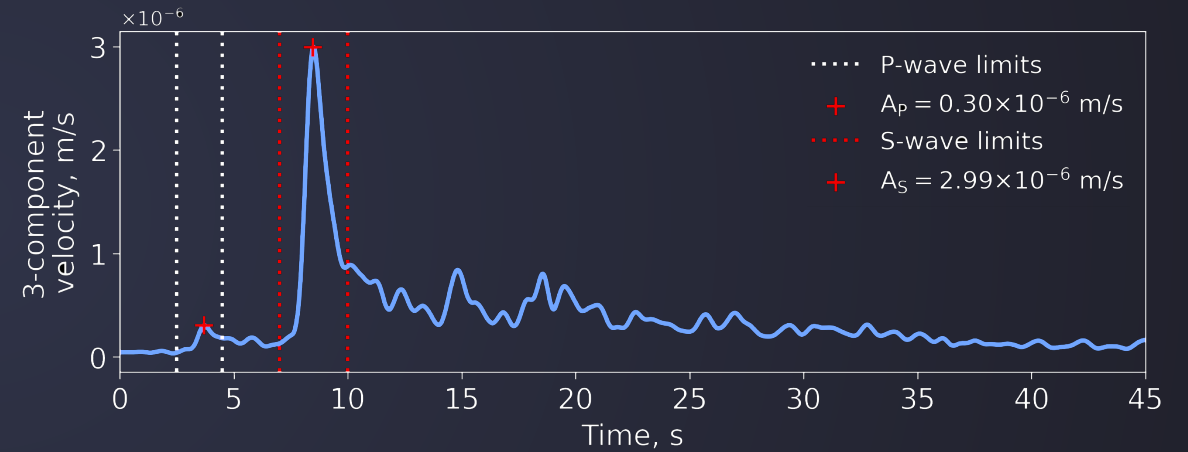
$$M_{L_1} = \frac{1}{N_{st}} \sum_{i=1}^{N_{st}} \Delta_i$$

Measuring real observed amplitudes



Computing the full amplitudes as:

$$A_{P,S} = \sqrt{(A_{P,S}^N)^2 + (A_{P,S}^E)^2 + (A_{P,S}^Z)^2}$$



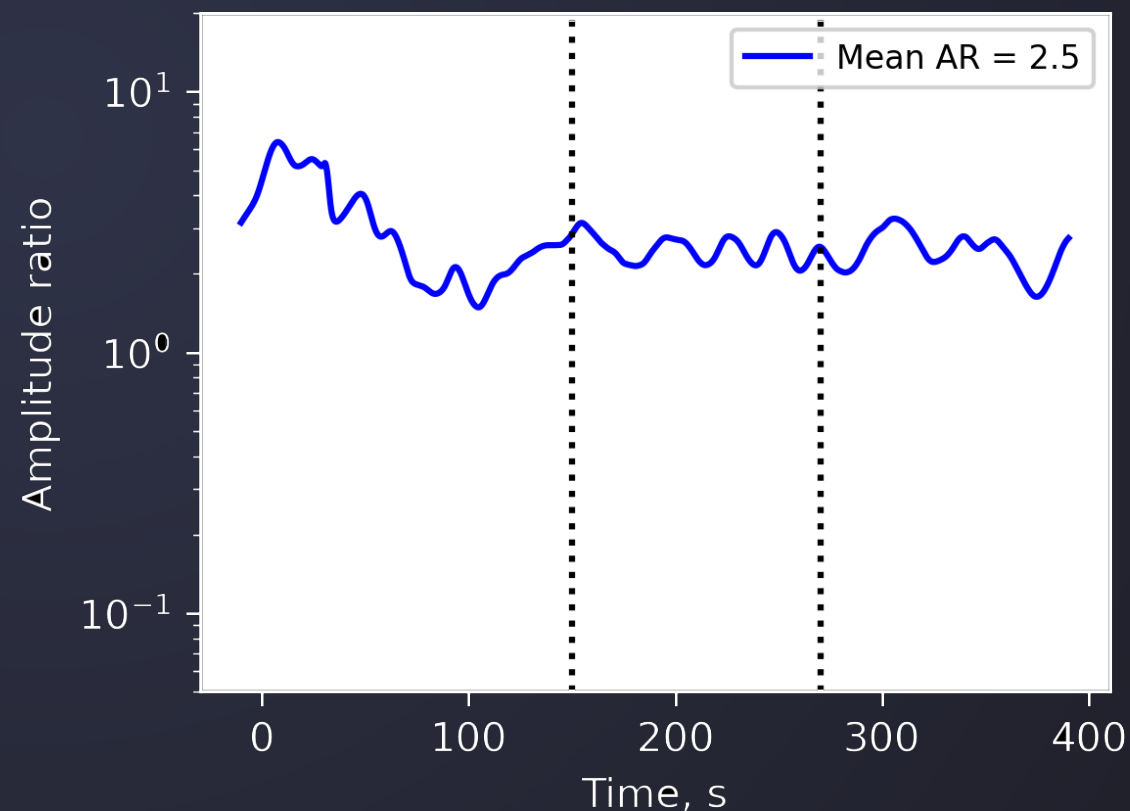
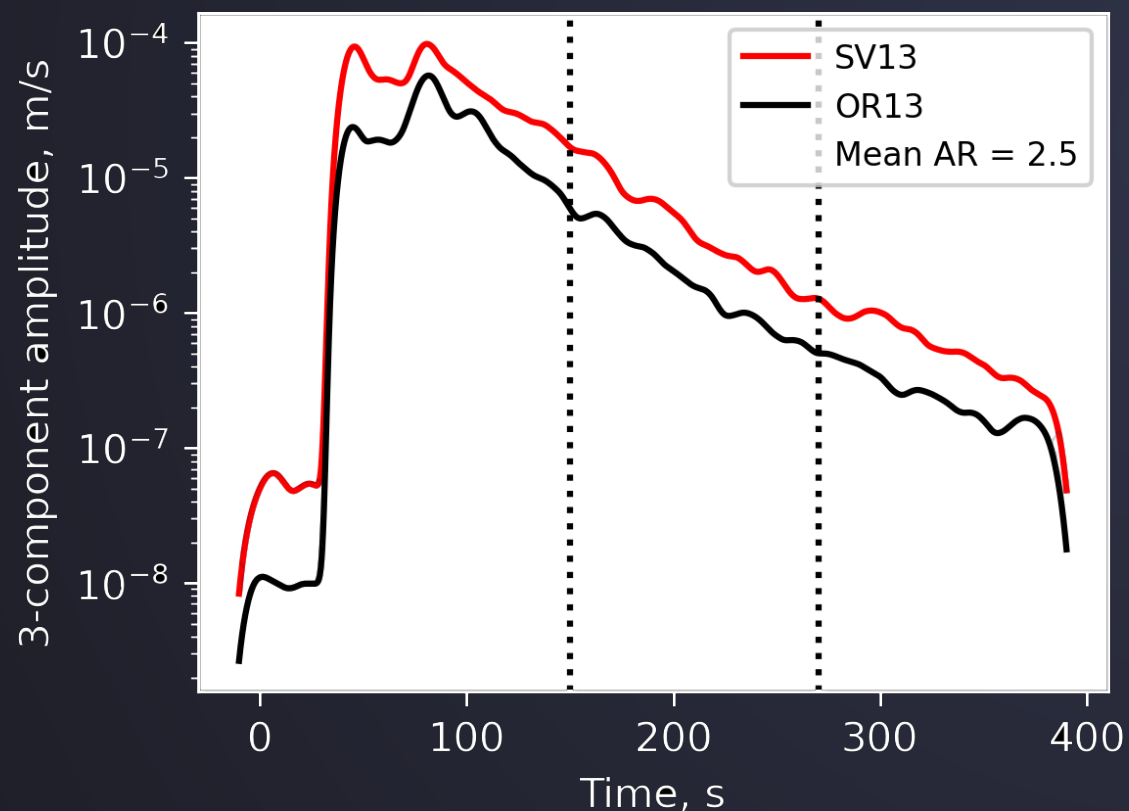
$$\left. \begin{array}{l} A_P = 0.3 \times 10^{-6} \text{ m/s} \\ A_S = 2.9 \times 10^{-6} \text{ m/s} \end{array} \right\} \frac{A_S}{A_P} = 9.9$$

This value is too high and cannot be produced by any of the considered source mechanisms !

Removing the site amplification effect

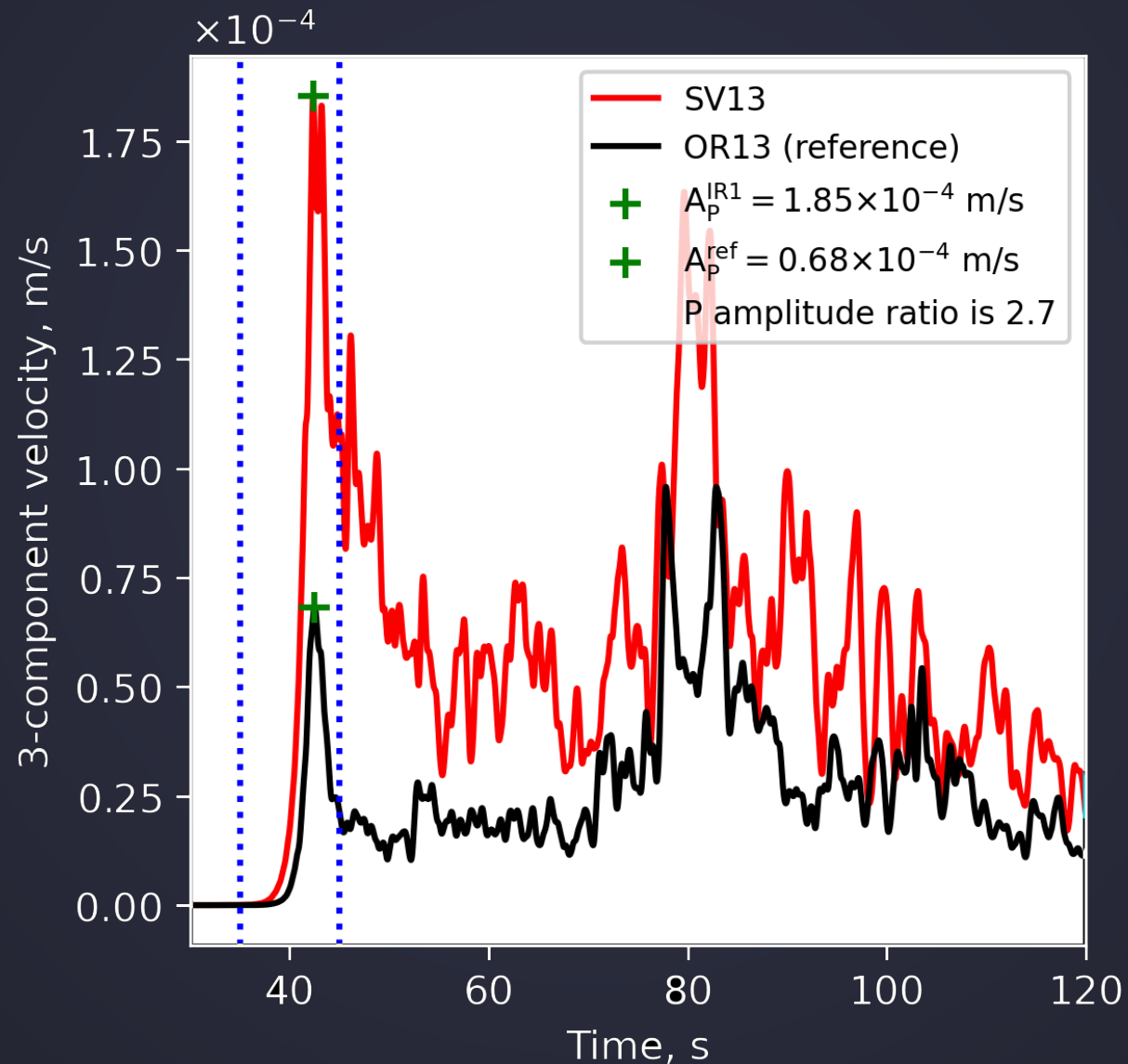
To remove the site effect for S-waves we used the method of **coda normalization**.

It is based on empirical observations that **coda waves consist of S-waves scattered at random heterogeneities in the earth.**



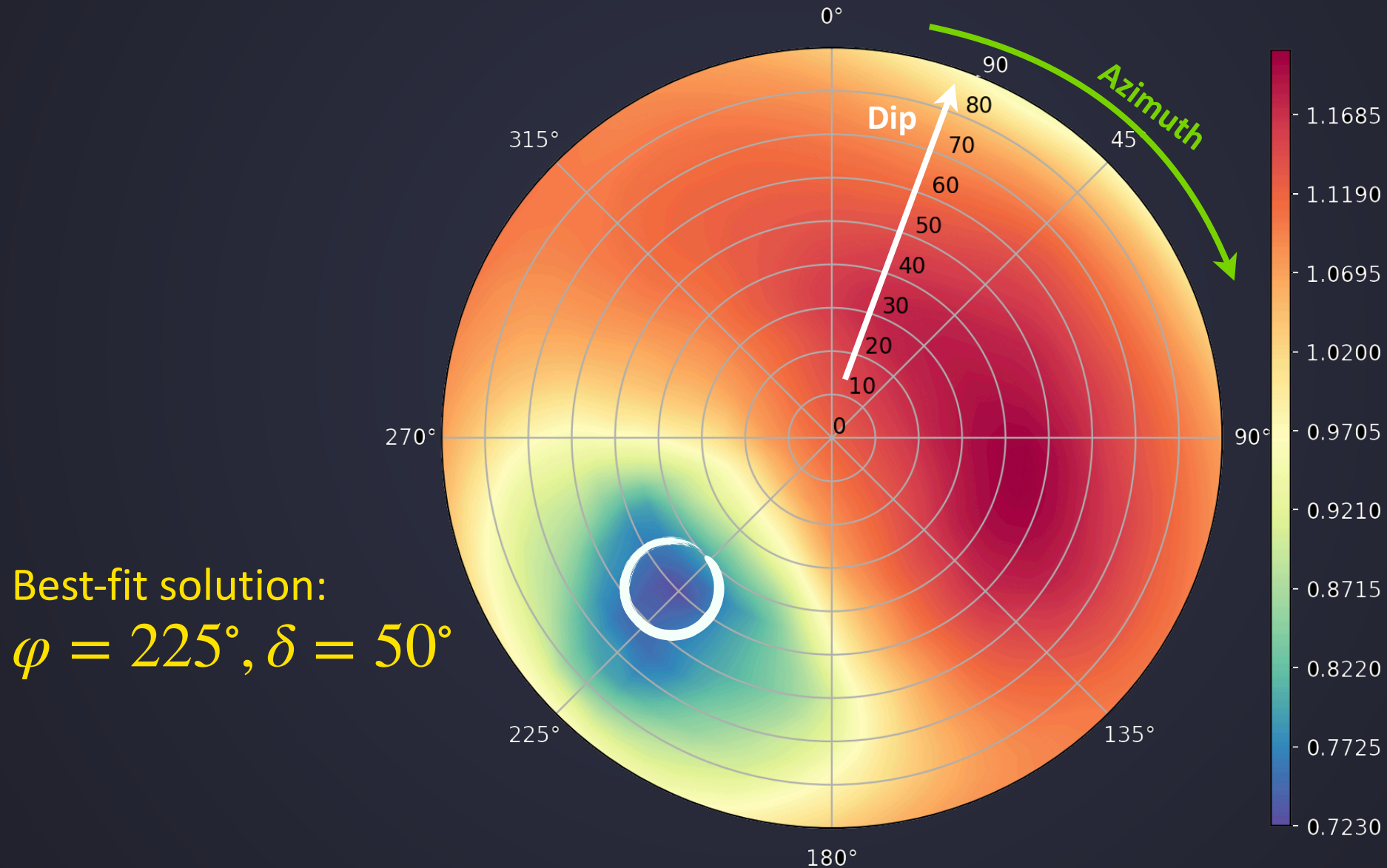
Removing the site amplification effect

For P-waves we simply picked the first arrivals



Results: example DLP on 20 August 2015 at 12:23:54

Misfit function distribution; combined source mechanism

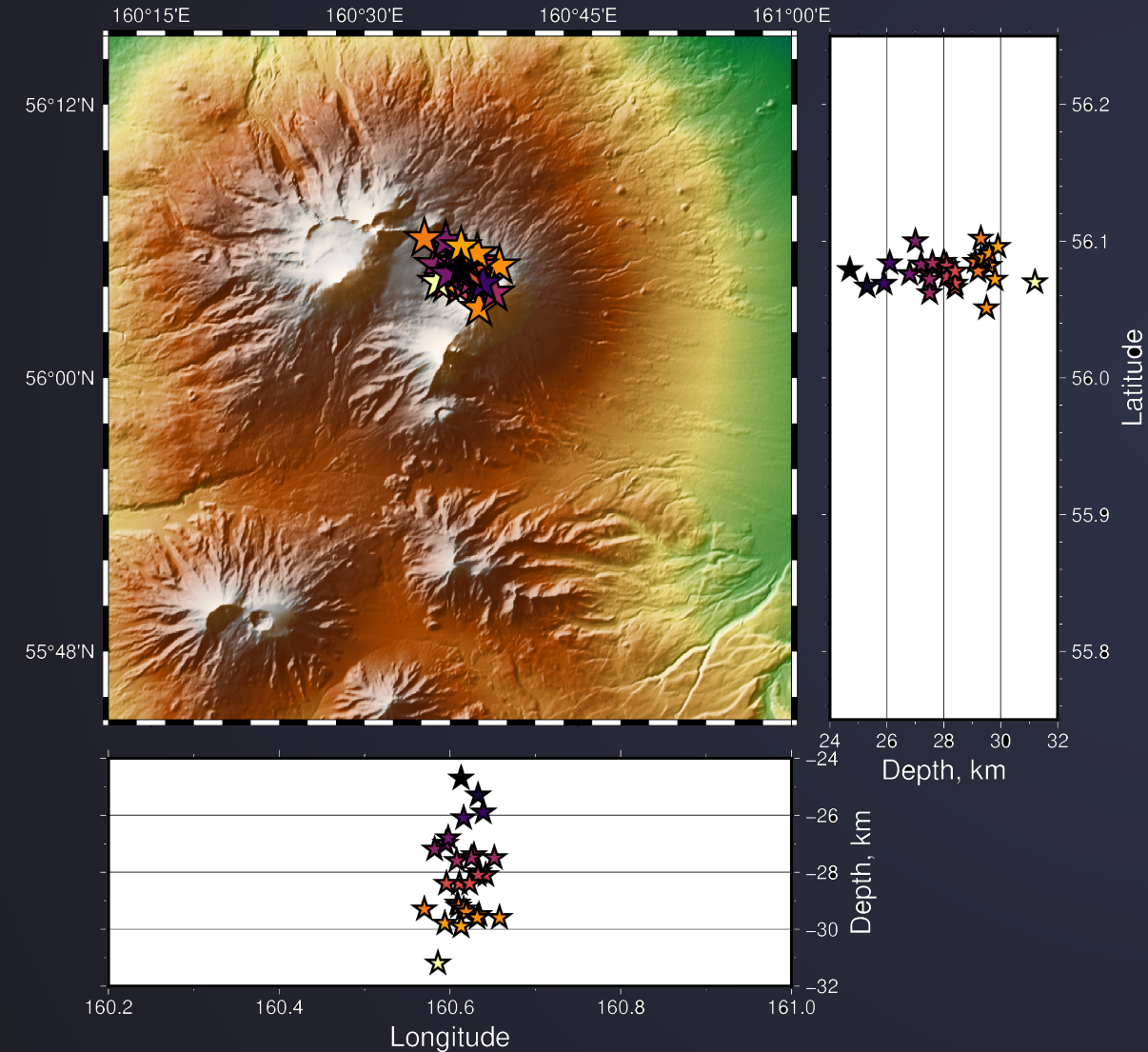


Results: example DLP on 20 August 2015 at 12:23:54

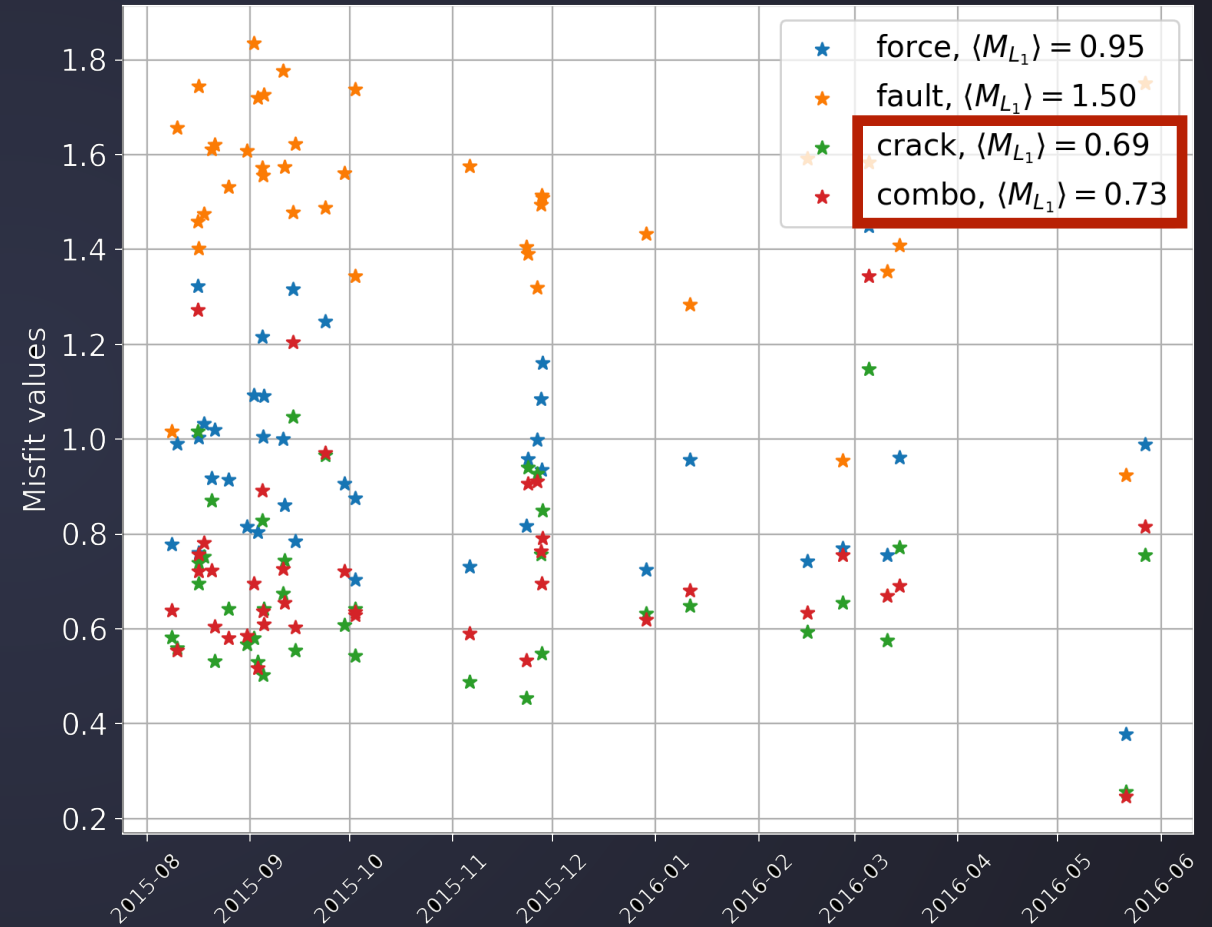
	Force	Shear slip	Tensile crack	Combined source
M_{L_1}	0.92	1.61	0.87	0.72
Source orientation	(220°, 40°)	(335°, 20°, 155°)	(275°, 20°)	(225°, 50°) $A_c : A_f = 1:2$

Massive processing

We selected 39 DLPs to perform the presented algorithm

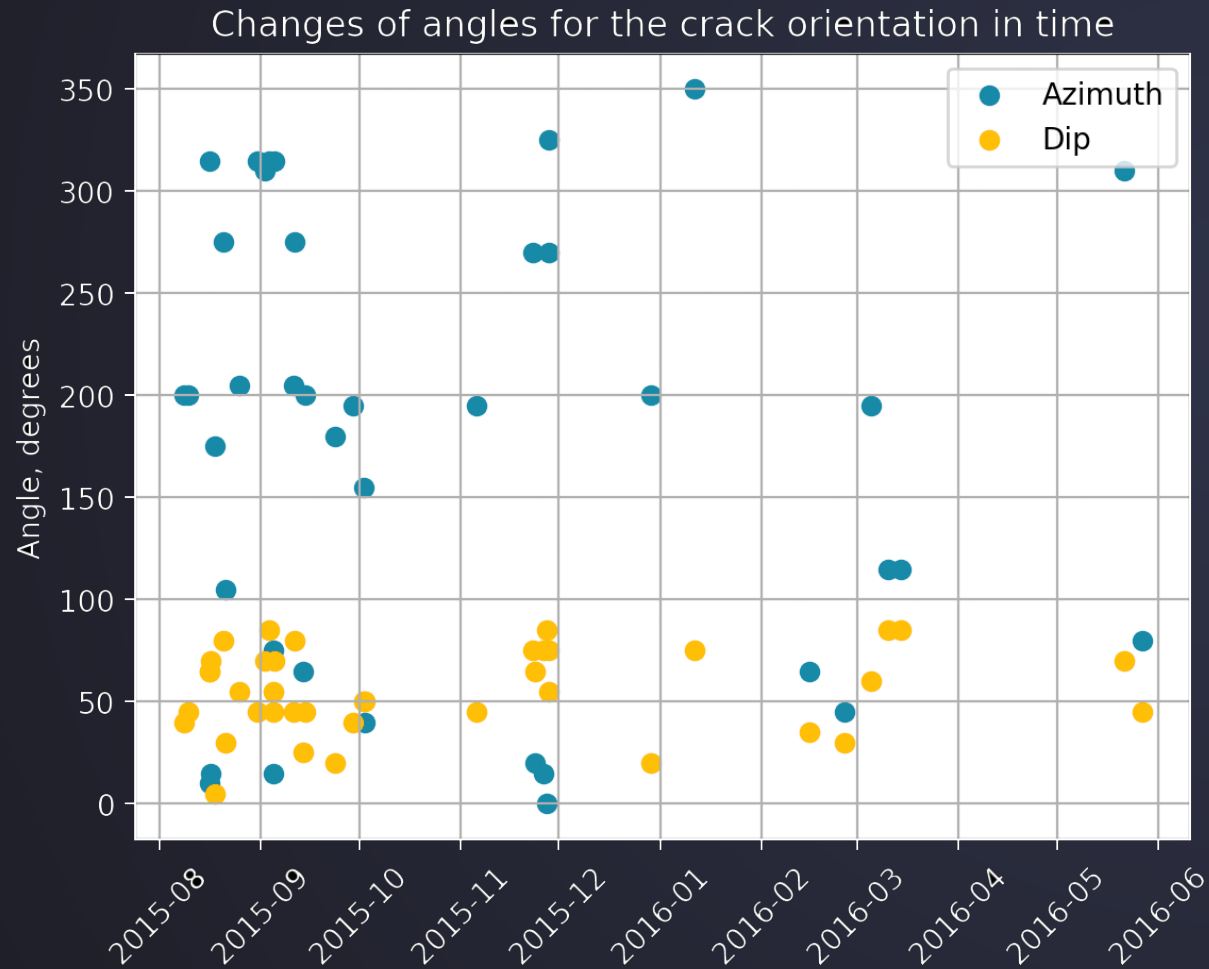


Distribution of misfit values in time



Massive processing

Although a tensile crack mechanism gives smaller misfit
the best fit solution is not very stable in time



The situation is better for **a combined source mechanism**

